Journal of Solid State Chemistry **159,** 68–71 (2001)
doi:10.1006/jssc.2001.9132, available online at http://www.idealibrary.com IDEAL®

Lithium Substitution in $LaMnO_3$: Synthesis, Structure, and Properties of $LaMn_{1-x}Li_xO_3$ Perovskites

Z. Serpil Gönen, J. Gopalakrishnan,[1] Scott A. Sirchio, B. W. Eichhorn, Vera Smolyaninova, and Richard L. Greene

Center for Superconductivity Research, Department of Physics and Department of Chemistry and Biochemistry, University of Maryland, College Park, Maryland 20742

Received October 23, 2000; in revised form January 31, 2001; accepted February 15, 2001; published online May 11, 2001

$LaMn_{1-x}Li_xO_3$ perovskites have been synthesized by a flux method using LiCl. Substitution of Li^+ creates mixed-valent manganese according to the formula $LaMn^{3+}_{1-3x}Mn^{4+}_{2x}Li^+_xO_3$, for $0.10 \leq x \leq 0.20$. At low values of x, additional vacancies are found on the perovskite A and B sites. All the members crystallize in the rhombohedral (R-3c) perovskite structure and are semiconducting with no long-range magnetic order. The samples show spin-glass-like short-range magnetic correlations at low temperatures and Curie–Weiss behavior above ca. 150 K. The $x = 0.05$ and 0.10 samples show a magnetoresistive effect of $\sim 90\%$ at 50 K and 8.5 T. The effect of Li^+ substitution in $LaMnO_3$ cannot be explained on the basis of a simple percolation model.

INTRODUCTION

Alkaline earth metal-substituted perovskite manganites, $Ln_{1-x}A_xMnO_3$ (Ln = La or rare earth; A = Ca, Sr, Ba), continue to attract attention in view of their exotic electronic properties that include colossal magnetoresistance, metal–insulator transition, and charge/orbital ordering (1, 2). Substitution of divalent A cations for the trivalent Ln in $LnMnO_3$ that creates a mixed-valent $Mn^{III/IV}O_3$ array in the perovskite structure is crucial for the occurrence of novel electronic properties in this family of oxides. Monovalent alkali cations have also been substituted for La in $LaMnO_3$, giving rise to similar Mn^{III}/Mn^{IV} mixed-valent compounds. These materials, with nominal formula $La_{1-x}A'_xMnO_3$ (A' = Na, K, Rb, Cs), show ferromagnetic and metallic properties although the structures are complicated by the presence of defects/vacancies at La/Mn or O sites (3–5). Interestingly, substitution of lithium in $LaMnO_3$ has not been reported to our knowledge. Considering the size (the Shannon radius of Li^+ in octahedral coordination is 0.76 Å), one would expect Li^+ to substitute at the octahedral B site in ABO_3 perovskites. Indeed, several B-site-substituted Li perovskites, such as A_2LiReO_6 (A = Ca, Sr, Ba) and La_2LiFeO_6, are known in the literature (6). Lithium is also known to substitute for copper in La_2CuO_4 (7) and $YBa_2Cu_3O_{6+y}$ (8), creating holes in CuO_2 planes that behave anomalously. Substitution of lithium at the A site of the ABO_3 perovskite structure is known in the rare instance of the lithium ion conductor, (La, Li) TiO_3 (9), although the exact location of lithium in this material appears to be unique (10).

We investigated the substitution of lithium at both the lanthanum and manganese sites of $LaMnO_3$. Although ordinary ceramic techniques did not give single-phase materials due to the formation of stable $LiMn_2O_4$, we could prepare single-phase $LaMn_{1-x}Li_xO_3$ using LiCl as flux. We describe the details of synthesis, structure, and properties of these new manganites in this paper.

EXPERIMENTAL

Our attempts to synthesize $LaMn_{1-x}Li_xO_3$ and $La_{1-x}Li_xMnO_3$ by reacting stoichiometric quantities of La_2O_3, Li_2CO_3, and MnO_2 at high temperatures did not yield single-phase products. A perovskite phase and $LiMn_2O_4$ were the major phases in the products and the latter persisted even beyond 1300°C. We could, however, prepare single-phase $LaMn_{1-x}Li_xO_3$ ($0 < x < 0.25$) by the following method using LiCl as flux. Stoichiometric quantities (10 mmoles, total) of La_2O_3 (predried at 950°C), Li_2CO_3, and MnO_2 corresponding to the formula $LaMn_{1-x}Li_xO_3$ for $0 < x < 0.25$ were mixed with 20 mmoles of LiCl. The mixture was heated slowly (100°C/h) to 1100°C/48 h and 1170°C/24 h with intermediate grinding. The product was thoroughly washed with distilled water until free from LiCl, dried at 110°C, pelletized, and the pellets were sintered at 1100°C/24 h. Powder X-ray diffraction patterns (XRD)

[1] On leave from the Solid State & Structural Chemistry Unit, Indian Institute of Science, Bangalore 560 012, India. To whom correspondence should be addressed.

0022-4596/01 $35.00

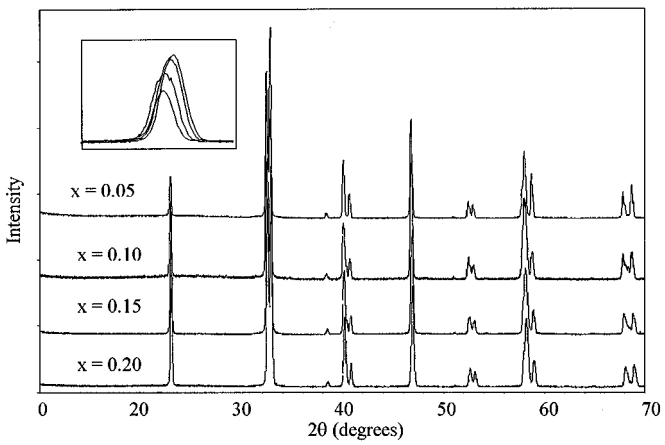

FIG. 1. XRD patterns for the $LaMn_{1-x}Li_xO_3$ samples where $x = 0.05$, 0.10, 0.15, and 0.20. The inset shows an enlarged view of the 0 1 2 reflection at $\sim 23^\circ$ for the $x = 0.2$ (top), 0.15, 0.10, and 0.05 (bottom) phases, respectively.

showed that the products were single-phase perovskite oxides (within the limits of detection of an XRD experiment). We could not, however, prepare $La_{1-x}Li_xMnO_3$ series by the LiCl flux method.

Chemical compositions of $LaMn_{1-x}Li_xO_3$ were determined by redox titrations (11) (Mn oxidation state), WDS analysis (La/Mn ratio), and ion chromatography (Li content). The redox titrations have a precision of $\pm 0.5\%$ (11). WDS analyses were performed using a JEOL microprobe analyzer with a single-crystal $La_{0.80}Ca_{0.20}MnO_{3.0}$ standard. XRD patterns (Fig. 1) were indexed on rhombohedral/hexagonal perovskite cells and the least-squares refined lattice parameters of $LaMn_{1-x}Li_xO_3$ members are listed in Table 1. Magnetization was measured from polycrystalline samples in gelatin capsules that were loaded into a SQUID magnetometer. Resistivity measurements were made by a standard four-probe technique on sintered pellets.

RESULTS

Synthesis and Structure

In Table 1, we give the chemical composition based on analytical results and lattice parameters of nominal $LaMn_{1-x}Li_xO_3$ members. We see that for $x \geq 0.10$, substitution of lithium occurs at the Mn site according to $4Mn^{3+} \rightarrow Li^+ + 2Mn^{4+} + Mn^{3+}$, giving the expected Mn^{4+} content. Accordingly, the formula of the solid solutions could be written as $LaMn^{3+}_{1-3x}Mn^{4+}_{2x}Li^+_xO_3$ for $0.10 \leq x \leq 0.20$. The $x = 0.05$ member has a considerably higher Mn^{4+} content than the expected $2x$ amount (Table 1). This result could be understood in terms of the following: undoped "$LaMnO_3$" synthesized under ambient atmosphere (i.e., an open container) is nonstoichiometric, containing about 20–25% of Mn^{4+} and 80–75% of Mn^{3+}, corresponding to the formula $La_{0.97}\square_{0.03}Mn^{3+}_{0.77}Mn^{4+}_{0.20}\square_{0.03}O_3$ where lattice vacancies ($\square$) occur at both La and Mn sites (12–15). Since our $LaMn_{1-x}Li_xO_3$ samples were prepared under ambient atmosphere, a higher Mn^{4+} content than that expected for $x = 0.05$ in nominal $LaMn_{1-x}Li_xO_3$ is consistent with the inherent tendency of manganese to oxidize to a $\sim 25\%$ $Mn^{4+}/75\%$ Mn^{3+} mixture in lanthanum manganite. Accordingly, we express the formula of the $x = 0.05$ member as $La_{0.98}\square_{0.02}Mn^{3+}_{0.72}Mn^{4+}_{0.21}Li^+_{0.05}\square_{0.02}O_3$ that is consistent with the chemical analysis results. A vacancy concentration of about 2% at both La and Mn sites is not unreasonable to expect considering that up to $\sim 5\%$ of La and Mn vacancies are known in oxidized $LaMnO_3$ (12–15).

All the $LaMn_{1-x}Li_xO_3$ members crystallize in the rhombohedral perovskite structure (Fig. 1, Table 1). There is a systematic decrease in the lattice parameters and cell volume, reflecting the increasing Mn^{4+} content with x. By comparison, oxidized $LaMnO_3$ samples containing $Mn^{4+} \geq 20\%$ adopt a rhombohedral (R-3c) structure (16). We believe the structure of $LaMn_{1-x}Li_xO_3$ reported here is similar to the rhombohedral structure of oxidized

TABLE 1
Chemical Composition and Lattice Parameters of $LaMn_{1-x}Li_xO_3$

	Total Mn (%)[a]		Mn^{4+}		WDS[c]		Lattice parameters		
x	Calcd	Obsd	(%)	Formula[b]	Calcd	Obsd	a_h (Å)	c_h (Å)	V (Å^3)
0.05	21.69	21.80	4.90	$La_{0.98}\square_{0.02}Mn^{3+}_{0.72}Mn^{4+}_{0.21}Li^+_{0.05}\square_{0.02}O_3$	0.93	0.926(7)	5.527(1)	13.321(2)	352.41
0.10	20.86	20.87	4.87	$LaMn^{3+}_{0.69}Mn^{4+}_{0.21}Li^+_{0.10}O_3$	0.90	0.888(7)	5.5241(8)	13.312(2)	351.79
0.15	19.90	19.93	7.05	$LaMn^{3+}_{0.55}Mn^{4+}_{0.30}Li^+_{0.15}O_3$	0.85	0.849(6)	5.5185(9)	13.290(9)	350.50
0.20	18.92	18.95	9.45	$LaMn^{3+}_{0.40}Mn^{4+}_{0.40}Li^+_{0.20}O_3$	0.80	0.797(9)	5.5121(9)	13.272(2)	349.21

[a] Calculated value based on the formula in this table.
[b] Formula based on Mn^{4+} content, reaction stoichiometry, and Li analysis.
[c] WDS is reported as the Mn : La ratio. The calculated value is based on the formula in this table.

TABLE 2
Magnetic and Transport Data for $LaMn_{1-x}Li_xO_3$ Oxides

Nominal x	θ (K)	μ(eff), obsd	μ(s–o), calcd	T_f (K)	E_a (eV)	ρ(295 K) (ohm cm)
0.05	165	5.8	4.7	70	0.13	1.3
0.10	140	5.6	4.7	50	0.13	4.3
0.15	122	5.2	4.6	30	0.14	6.8
0.20	97	5.0	4.4	25	0.14	24

$LaMnO_3$, where Li^+ ions are randomly distributed at the Mn sites.

Electrical Transport and Magnetic Properties

The direct current magnetic susceptibility of polycrystalline $LaMn_{1-x}Li_xO_3$ samples was measured between 5 K and 300 K using a SQUID magnetometer. A summary of the magnetic data is given in Table 2. The field-cooled (FC) and zero-field-cooled (ZFC) susceptibilities of the $x = 0.05$ member (Fig. 2) show spin-glass-like behavior with short-range ordering below 128 K. The $x = 0.10$, 0.15, and 0.20 samples also show similar spin-glass-like behavior with freezing temperatures (T_f) shifting to lower values of 100, 60, and 25 K, respectively. Above T_f, the samples exhibit a Curie–Weiss-like behavior (see Fig. 3) but the data are not rigorously linear at any temperature. The approximated temperature intercepts in the paramagnetic region decrease progressively from 165 K ($x = 0.05$) to 97 K ($x = 0.20$). As expected, the susceptibility steadily decreases with Li^+ content due to the associated increase of Mn^{4+} (d^3) at the expense of Mn^{3+} (high-spin d^4). The magnetic moments (per Mn ion) in the paramagnetic region were estimated from the

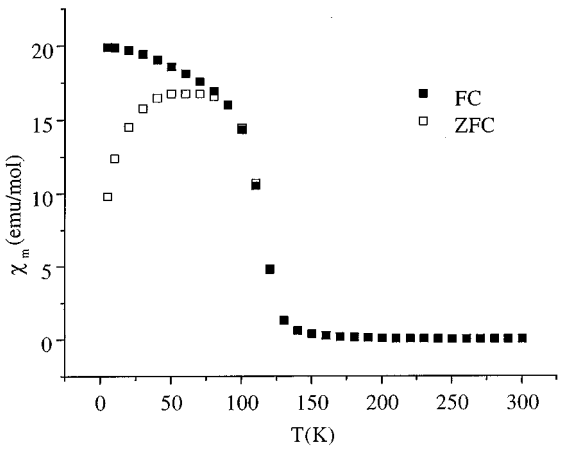

FIG. 2. Field-cooled (FC) and zero-field-cooled (ZFC) molar magnetic susceptibility for the $x = 0.05$ sample in the $LaMn_{1-x}Li_xO_3$ series. Data were recorded at 100 Oe.

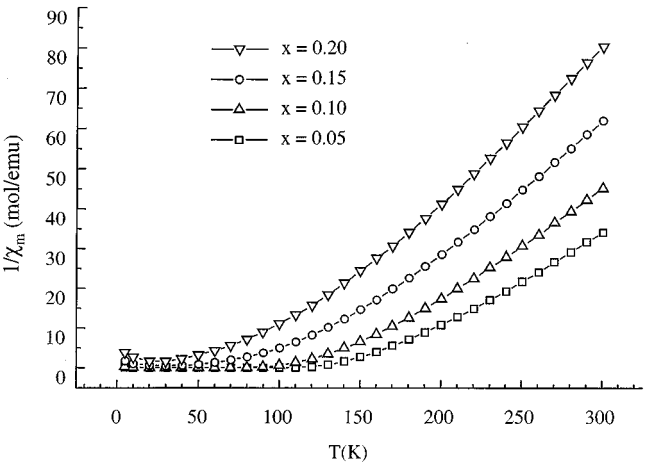

FIG. 3. Plots of reciprocal molar susceptibility versus temperature for the $LnMn_{1-x}Li_xO_3$ samples.

equation

$$\chi_m = \frac{Ng^2\beta^2 S(S+1)}{3k(T-\theta)}.$$

The moments are all listed in Table 2 and are significantly greater than the values for the chemical formulas given in Table 1. The deviations from the spin-only values in this region are most likely due to existence of superparamagnetic clusters where the double-exchange ferromagnetic interaction between Mn^{3+}/Mn^{4+} is stronger than the antiferromagnetic interaction. The long-range interactions, however, are suppressed by the random disorder introduced by the Li^+ ions which lead to the observed spin-glass-like behavior at lower temperatures. A similar behavior and explanation have been reported for nonstoichiometric lanthanum manganites (15, 17, 18).

The electrical resistivity measurements (Fig. 4) show that all samples are semiconducting with room temperature

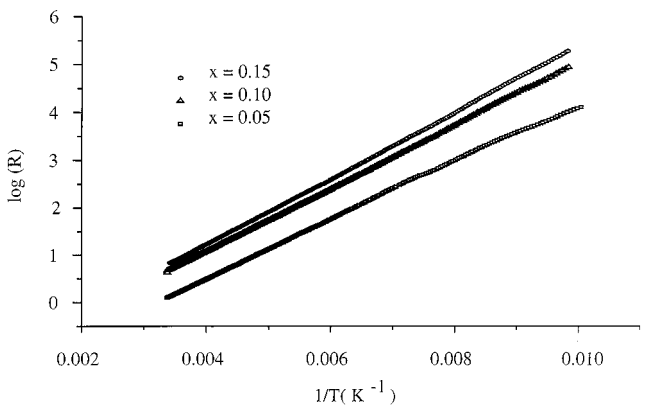

FIG. 4. Plot of $\log(R)$ vs $1/T$ for the $LaMn_{1-x}Li_xO_3$ samples.

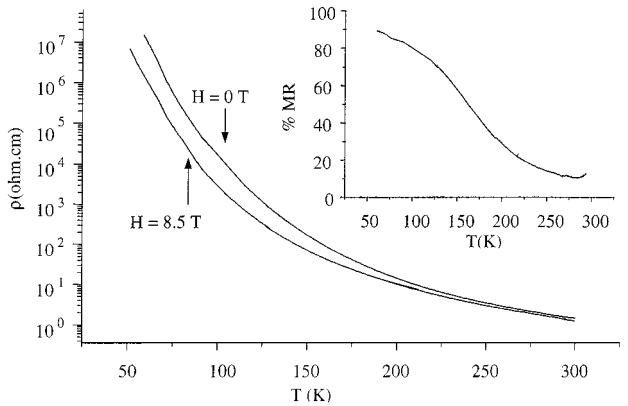

FIG. 5. Temperature dependence of resistivity for $LaMn_{0.95}Li_{0.05}O_3$ recorded at 8.5 Tesla and in the absence of field. The inset shows the magnetoresistance of the sample. $\%MR = [\rho(0\,T) - \rho(8.5\,T)]/\rho(0\,T) \times 100$.

resistivities increasing with increasing Li content. The activation energies are similar at ~ 0.13 eV (Table 2). The magnetoresistivity of the $x = 0.05$ sample was measured at 8.5 T (Fig. 5) but showed only a modest response (90%) at 50 K. A similar magnetoresistance is observed for the $x = 0.10$ sample.

DISCUSSION

All the samples are semiconductors/insulators with no long-range (ferro) magnetic ordering. Significantly, even the $x = 0.05$ sample where 93% of the sites are occupied by manganese ($\sim 0.21\,Mn^{4+}/0.72\,Mn^{3+}$) is semiconducting with no long-range magnetic ordering. The results indicate that a substitution of about 5–7% of manganese sites by lithium or Mn vacancies is sufficient to disrupt the long-range magnetic ordering, rendering the samples semiconducting. It is well known that $La_{1-x}A_xMnO_3$ materials containing an equivalent amount of Mn^{4+}/Mn^{3+} (≤ 0.30) exhibit ferromagnetic and metallic properties. According to percolation theory (19, 20), the percolation threshold, p, for site substitution in a perovskite lattice is 0.31. This means that a substitution of less than 69% of Mn sites in $LaMnO_3$ would still preserve the connectivity of Mn–O–Mn bonds and therefore one would expect long-range electrical and magnetic properties consistent with Mn^{3+}/Mn^{4+} content. But our experimental results on $LaMn_{1-x}Li_xO_3$ suggest that the effect of lithium substitution cannot be understood on the basis of a simple percolation model. It is possible that an Anderson-type localization (21) could be responsible for the semiconducting behavior due to the introduction of impurity states (Li^+) directly into the conduction band.

ACKNOWLEDGMENTS

We gratefully acknowledge the National Science Foundation (NSF-DMR 0076460) and the Department of Science and Technology, Government of India (J.G.), for support of this work.

REFERENCES

1. Y. Tokura and N. Nagosa, *Science* **288,** 462 (2000).
2. Y. Tokura, "Colossal Magnetoresistive Oxides," p. 200. Gordon and Breach Science, New York, 2000.
3. T. Boix, F. Sapina, Z. El-Fadli, E. Martinez, A. Beltram, J. Vergara, R. J. Ortega, and K. V. Rao, *Chem. Mater.* **10,** 1569 (1998).
4. Y. Ng-Lee, F. Sapina, E. Martinez-Tamayo, J.-V. Folgado, R. Ibanez, D. Beltran, F. Lloret, and A. Segura, *J. Mater. Chem.* **7,** 1905 (1997).
5. K. Ramesha, V. N. Smolyaninova, J. Gopalakrishnan, and R. L. Greene, *Chem. Mater.* **10,** 1436 (1998).
6. M. T. Anderson, K. B. Greenwood, G. A. Taylor, and K. R. Poeppelmaier, *Prog. Solid State Chem.* **22,** 197 (1993).
7. W. Bao, R. J. McQueeney, R. Heffner, J. L. Sarrao, P. Dai, and J. L. Zarestky, *Phys. Rev. Lett.* **84,** 3978 (2000).
8. J. Bobroff, W. A. MacFarlane, H. Alloul, P. Mendels, N. Blanchard, G. Collin, and J. F. Marucco, *Phys. Rev. Lett.* **83,** 4381 (1999).
9. Y. Inaguma, L. Chen, M. Itoh, T. Nakamura, T. Uchida, M. Ikuta, and M. Wakihara, *Solid State Commun.* **86,** 689 (1993).
10. J. A. Alonso, J. Sanz, J. Santamaria, C. Leon, A. Varez, and M. T. Fernandex-Diaz, *Angew. Chem., Int. Ed.* **39,** 619 (2000).
11. J. Bloom, E. T. Y. Kometani, and J. W. Mitchell, *J. Inorg. Nucl. Chem.* **40,** 403 (1978).
12. M. Hervieu, R. Mahesh, N. Rangavittal, and C. N. R. Rao, *Eur. J. Solid State Inorg. Chem.* **32,** 79 (1995).
13. Q. Huang, A. Santoro, J. W. Lynn, R. W. Erwin, J. A. Borchers, J. L. Peng, and R. L. Greene, *Phys. Rev. B* **55,** 14987 (1997).
14. J. A. M. v. Roosmalen and E. H. P. Cardfunke, *J. Solid State Inorg. Chem.* **32,** 79 (1994).
15. J. Töpfer and J. B. Goodenough, *J. Solid State Chem.* **130,** 117 (1997).
16. C. Ritter, M. R. Ibarra, J. M. DeTeresa, P. A. Algarabel, C. Marquina, J. Blasco, J. Garcia, S. Oseroff, and S. W. Cheong, *Phys. Rev. B* **56,** 8902 (1997).
17. L. Ghivelder, I. Abergo Castillo, M. A. Gusmao, J. A. Alonso, and L. F. Cohen, *Phys. Rev. B* **60,** 12184 (1999).
18. J. Töpfer and J. B. Goodenough, *Chem. Mater.* **9,** 1467 (1997).
19. V. K. S. Shante and S. Kirkpatrick, *Adv. Phys.* **20,** 325 (1971).
20. D. Stauffer, "Introduction to Percolation Theory." Taylor & Francis, London, 1985.
21. P. W. Anderson, *Phys. Rev.* **109,** 1492 (1958).